

Nondegenerate two-mode squeezing and quantum-nondemolition measurements using three-level atoms in a cavity

J. Ph. Poizat,* M. J. Collett, and D. F. Walls

Physics Department, University of Auckland, Auckland, New Zealand

(Received 26 August 1991)

We consider two modes of the electromagnetic field interacting via a three-level atom in a ladder configuration. We calculate the squeezing spectra of the sum and difference of the two output beams. The usefulness of this system as a quantum-nondemolition-measurement scheme is analyzed and a prediction is made using the parameters of a recent experiment by Grangier *et al.* [Phys. Rev. Lett. **66**, 1418 (1991)]. We use a full three-level model in the most general case and in particular the influence of both the one-photon and the two-photon detunings are investigated.

PACS number(s): 42.50.Lc, 42.50.Dv

I. INTRODUCTION

There have been a number of schemes proposed for quantum-nondemolition (QND) measurements [1] in optics [2-9]. These have resulted in several experimental demonstrations by Levenson *et al.* [10], La Porta *et al.* [11], and Grangier *et al.* [12]. It is the experiment of Grangier *et al.* which we wish to analyze in this paper. Their experiment is based on the coupling of two cavity-electromagnetic-field modes via a two-photon transition in a three-level atom in a ladder configuration. The phase fluctuations of the probe field are correlated with the amplitude fluctuations of the signal field via the nonlinear interaction. An analysis of this system was given by Grangier *et al.* [8] in the dispersive limit where spontaneous emission from the atoms was neglected. An analysis which included spontaneous emission from the atoms was given by Blockley and Walls [9]. They used an effective two-level atomic model which assumed the intermediate level is highly detuned from the optical frequencies. Thus, only the influence of the two-photon detuning was considered.

In this paper we treat a full three-level atomic model which enables us to include the influence of the one-photon detuning in addition to the two-photon detuning. For large one-photon detuning we recover the results obtained using the effective two-level-atom model. We use the criteria given by Holland *et al.* [13] to evaluate this scheme as a QND measurement. In particular, we evaluate the QND capability of this scheme for the range of parameters accessible in the experiment of Grangier *et al.* In addition, we calculate the squeezing in the sum and the difference of the two output beams. We are able to extend some previous results based on an effective two-level model of the atomic medium [14].

II. PRINCIPLE OF THE CALCULATION

We wish to describe the interaction of two cavity modes of the electromagnetic field coupled via a two-photon transition in an ensemble of three-level atoms in a ladder configuration as shown in Fig. 1. The atomic tran-

sitions and the field modes are coupled to thermal baths taken to be in the vacuum state. The Hamiltonian describing this interaction can be split into four terms:

$$H = H_1 + H_2 + H_3 + H_4 + H_{\text{baths}} \quad (1)$$

H_1 is the free part of the Hamiltonian for the atoms as well as for the field modes, H_2 is the atom-field-coupling part of the Hamiltonian, H_3 describes the damping of the cavity modes by the coupling with the field bath, and H_4 the damping of the atoms by spontaneous emission. H_{baths} is the Hamiltonian for all the different baths. The rotating-wave approximation is made. We have

$$\begin{aligned} H_1 &= \sum_{\mu=1}^N \sum_{i=1}^3 \hbar v_i \sigma_{ii}^{\mu} + \sum_{j=1}^2 \hbar \omega_j a_j^{\dagger} a_j, \\ H_2 &= i \hbar g_1 \sum_{\mu=1}^N (a_1^{\dagger} \sigma_{12}^{\mu} e^{ik_1^{\mu} r^{\mu}} - \text{H.c.}) \\ &\quad + i \hbar g_2 \sum_{\mu=1}^N (a_2^{\dagger} \sigma_{23}^{\mu} e^{ik_2^{\mu} r^{\mu}} - \text{H.c.}), \\ H_3 &= i \hbar \sum_{j=1}^2 \int_{-\infty}^{\infty} d\omega C_j(\omega) [b^{\dagger}(\omega) a_j - \text{H.c.}], \\ H_4 &= i \hbar \sum_{\mu=1}^N (\Gamma_1^{\dagger} \sigma_{12}^{\mu} - \text{H.c.}) + i \hbar \sum_{\mu=1}^N (\Gamma_2^{\dagger} \sigma_{23}^{\mu} - \text{H.c.}). \end{aligned} \quad (2)$$

In these equations, σ_{kl} are, respectively, the populations and the coherences, a_j and a_j^{\dagger} are the boson operators for each field mode, $\hbar v_i$ is the energy level of the i th atomic level, ω_j is the frequency of the mode j of the cavity. g_1 and g_2 are the coupling constants for the lower and upper transition, respectively (taken as real). k_j is the wave vector of the mode j , r^{μ} is the position of the μ th atom, and a phase term $e^{ik_j r_j^{\mu}}$ takes into account the position of each individual atom. b_j and b_j^{\dagger} are the boson operators for the field bath. Γ_j and Γ_j^{\dagger} are the atomic bath operators for each transition ($j=1,2$). The commutation relations for the different operators are

$$[a_j, a_{j'}^{\dagger}] = \delta_{jj'}, \quad (3)$$

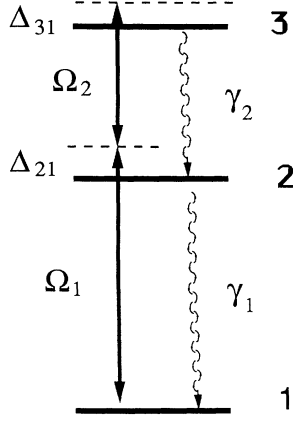


FIG. 1. Scheme of the three-level system.

and

$$[b_j(\omega), b_{j'}(\omega')] = \delta_{jj'} \delta(\omega - \omega'). \quad (4)$$

The multiplication rules for the atomic operators are

$$\sigma_{ij}^\mu \sigma_{kl}^\mu = \delta_{jk} \sigma_{il}^\mu. \quad (5)$$

$C_j(\omega)$ is the coupling coefficient between the bath and the inside modes and is assumed to be constant over a broadband of frequencies about each characteristic frequency Ω_j . We then have $C_j(\omega)^2 = \kappa_j / 2\pi$, where κ_j is the cavity decay rate.

We shall take a_j and b_j to be in the frame rotating at the frequency Ω_j of the corresponding driving field ($j=1,2$). We define the input fields by (see Ref. [15] for more details)

$$a_j^{\text{in}}(t) = \frac{1}{\sqrt{2\pi}} \int_{-\infty}^{\infty} d\omega e^{-i\omega(t-t_0)} b_j^0(\omega) \quad \text{for } t > t_0, \quad (6)$$

where $b_j^0(\omega)$ is the value of $b_j(\omega)$ at $t=t_0$.

We define atomic operators for the whole atomic system:

$$\begin{aligned} S_{ii} &= \sum_{\mu=1}^N \sigma_{ii}^\mu, \\ S_{12} &= \sum_{\mu=1}^N \sigma_{12}^\mu e^{-ik_1 r^\mu}, \\ S_{23} &= \sum_{\mu=1}^N \sigma_{23}^\mu e^{-ik_2 r^\mu}, \\ S_{13} &= \sum_{\mu=1}^N \sigma_{13}^\mu e^{-i(k_1+k_2)r^\mu}, \end{aligned} \quad (7)$$

and similar obvious definitions for S_{21} , S_{32} , and S_{31} .

We can now write down the Heisenberg equations of motion for the whole set of operators, in the frames rotating at Ω_1 and Ω_2 . We obtain ($j=1,2$ corresponding to the two field modes)

$$\frac{da_j}{dt} = -\kappa_j(1+i\Phi_j)a_j + g_j S_{jj+1} - \sqrt{2\kappa_j} a_j^{\text{in}}, \quad (8)$$

$$\begin{aligned} \frac{dS_{11}}{dt} &= \gamma_1 S_{22} + g_1(S_{21}a_1 + a_1^\dagger S_{12}) \\ &\quad + \sqrt{\gamma_1} \sum_{\mu=1}^N (\sigma_{21}^\mu \beta_1^{\text{in}} + \beta_1^{\text{in}\dagger} \sigma_{12}^\mu), \end{aligned} \quad (9)$$

$$\begin{aligned} \frac{dS_{33}}{dt} &= -\gamma_2 S_{33} - g_2(S_{32}a_2 + a_2^\dagger S_{23}) \\ &\quad - \sqrt{\gamma_2} \sum_{\mu=1}^N (\sigma_{32}^\mu \beta_2^{\text{in}} + \beta_2^{\text{in}\dagger} \sigma_{23}^\mu), \end{aligned} \quad (10)$$

$$\begin{aligned} \frac{dS_{12}}{dt} &= -\frac{\gamma_1}{2}(1+i\Delta_{21})S_{12} + g_1 a_1(S_{22} - S_{11}) + g_2 a_2^\dagger S_{13} \\ &\quad + \sqrt{\gamma_1} \sum_{\mu=1}^N (\sigma_{22}^\mu - \sigma_{11}^\mu) \beta_1^{\text{in}} e^{-ik_1 r^\mu} \\ &\quad + \sqrt{\gamma_2} \sum_{\mu=1}^N \beta_2^{\text{in}\dagger} \sigma_{13}^\mu e^{-ik_1 r^\mu}, \end{aligned} \quad (11)$$

$$\begin{aligned} \frac{dS_{23}}{dt} &= -\frac{1}{2}(\gamma_1 + \gamma_2)(1+i\Delta_{32})S_{23} \\ &\quad - g_1 a_1^\dagger S_{13} + g_2 a_2(S_{33} - S_{22}) \\ &\quad - \sqrt{\gamma_1} \sum_{\mu=1}^N \beta_1^{\text{in}\dagger} \sigma_{13}^\mu e^{-ik_2 r^\mu} \\ &\quad + \sqrt{\gamma_2} \sum_{\mu=1}^N (\sigma_{33}^\mu - \sigma_{22}^\mu) \beta_2^{\text{in}} e^{-ik_2 r^\mu}, \end{aligned} \quad (12)$$

$$\begin{aligned} \frac{dS_{13}}{dt} &= -\frac{\gamma_2}{2}(1+i\Delta_{31})S_{13} + g_1 a_1 S_{23} - g_2 a_2 S_{12} \\ &\quad + \sqrt{\gamma_1} \sum_{\mu=1}^N \sigma_{23}^\mu \beta_1^{\text{in}} e^{-i(k_1+k_2)r^\mu} \\ &\quad - \sqrt{\gamma_2} \sum_{\mu=1}^N \sigma_{12}^\mu \beta_2^{\text{in}} e^{-i(k_1+k_2)r^\mu}, \end{aligned} \quad (13)$$

and

$$S_{11} + S_{22} + S_{33} = N, \quad (14)$$

together with the other three obvious equations for the conjugate variables. We have defined the scaled atom-laser detunings

$$\begin{aligned} \Delta_{21} &= [(\nu_2 - \nu_1) - \Omega_1] / (\gamma_1/2), \\ \Delta_{32} &= [(\nu_3 - \nu_2) - \Omega_2] / [(\gamma_1 + \gamma_2)/2], \end{aligned}$$

and

$$\Delta_{31} = [(\nu_3 - \nu_2) - (\Omega_1 + \Omega_2)] / (\gamma_2/2), \quad (15)$$

and $\phi_j = (\omega_j - \Omega_j) / \kappa_j$ are the scaled empty-cavity detunings.

The deterministic mean values of the atomic variables in the steady state can be found by setting the time derivatives to zero and neglecting the noise terms. This involves solving the eight coupled linear equations for the atomic variables. This enables us to obtain a relation between the mean values of the input- and internal-field operators. We have, for $j=1,2$,

$$\langle a_j^{\text{in}} \rangle = -[\kappa_j(1+i\Phi_j)\langle a_j \rangle - g_j \langle S_{jj+1} \rangle] / \sqrt{2\kappa_j}. \quad (16)$$

We define the phases θ_j^{in} by

$$\frac{\langle a_j^{\text{in}} \rangle}{|\langle a_j^{\text{in}} \rangle|} = \frac{\langle a_j \rangle}{|\langle a_j \rangle|} e^{i\theta_j^{\text{in}}}. \quad (17)$$

Using the boundary condition for the input-output formalism [15] for $j=1,2$,

$$a_j^{\text{out}}(t) - a_j^{\text{in}}(t) = \sqrt{2\kappa_j} a_j, \quad (18)$$

we have analogous relations for the output operators in terms of the internal operators

$$\langle a_j^{\text{out}} \rangle = -[\kappa_j(-1+i\Phi_j)\langle a_j \rangle - g_j \langle S_{jj+1} \rangle] / \sqrt{2\kappa_j} \quad (19)$$

and

$$\frac{\langle a_j^{\text{out}} \rangle}{|\langle a_j^{\text{out}} \rangle|} = \frac{\langle a_j \rangle}{|\langle a_j \rangle|} e^{-i\theta_j^{\text{out}}}. \quad (20)$$

These phases are important when we deal with a specific output quadrature.

Expressing $\langle S_{12} \rangle$ and $\langle S_{23} \rangle$ in terms of $\langle S_{13} \rangle$, using Eqs. (11) and (12) without the noise terms and the time derivatives, and inserting these quantities back in Eq. (13), we obtain (for the mean value)

$$\begin{aligned} 0 = & -\frac{\gamma_2}{2}(1+i\Delta_{31})\langle S_{13} \rangle - \frac{g_1^2}{\frac{1}{2}(\gamma_1+\gamma_2)(1+i\Delta_{32})}\langle a_1 \rangle \langle a_1^\dagger \rangle \langle S_{13} \rangle - \frac{g_2^2}{(\gamma_1/2)(1+i\Delta_{21})}\langle a_2 \rangle \langle a_2^\dagger \rangle \langle S_{13} \rangle \\ & + \frac{g_1 g_2}{\frac{1}{2}(\gamma_1+\gamma_2)(1+i\Delta_{32})}\langle a_1 \rangle \langle a_2 \rangle (\langle S_{33} \rangle - \langle S_{22} \rangle) - \frac{g_1 g_2}{(\gamma_2/2)(1+i\Delta_{21})}\langle a_1 \rangle \langle a_2 \rangle (\langle S_{22} \rangle - \langle S_{11} \rangle). \end{aligned} \quad (21)$$

If $|\Delta_{32}| \gg 1$ and $|\Delta_{32}| \gg |\Delta_{31}|$, we have $\frac{1}{2}(\gamma_1+\gamma_2)\Delta_{32} \sim -(\gamma_2/2)\Delta_{21} = \delta$ and the last equation becomes

$$0 = -\frac{\gamma_2}{2}(1+i\Delta'_{31})\langle S_{13} \rangle + g \langle a_1 a_2 \rangle (\langle S_{33} \rangle - \langle S_{11} \rangle), \quad (22)$$

where $g = g_1 g_2 / i\delta$ and

$$\Delta'_{31} = \Delta_{31} - \frac{2}{\gamma_2} \frac{g_1^2 \langle a_1 \rangle \langle a_1^\dagger \rangle}{\delta} + \frac{2}{\gamma_2} \frac{g_2^2 \langle a_2 \rangle \langle a_2^\dagger \rangle}{\delta}$$

is the two-photon detuning corrected by the Stark shifts of, respectively, the ground and the upper level [16] (which are of order of magnitude $\sim \gamma_2$ for the type of parameters we are considering here, but cancel each other if $g_1 \langle a_1 \rangle = g_2 \langle a_2 \rangle$). So if we neglect the Stark shifts, we recover the same equation we obtained with the effective two-level-atom model of our previous publication [14].

Provided that the fluctuations are small enough compared to the deterministic mean values, we can linearize each variable about its mean value:

$$\begin{aligned} a_j &= \langle a_j \rangle + \delta a_j \quad \text{for } j=1,2, \\ S_{kl} &= \langle S_{kl} \rangle + \delta S_{kl} \quad \text{for } k,l=1,2,3. \end{aligned} \quad (23)$$

Let us define a scaled atomic noise for the system, $B_j^{\text{in}} = 1/\sqrt{N} \sum_{\mu=1}^N B_j^{\text{in}} e^{-ik_j r^\mu}$, for $j=1,2$. We can now write the equations of motion for the fluctuation operators. We have

$$\begin{aligned} \frac{d}{dt} \delta a_j &= -\kappa_j(1+i\Phi_j)\delta a_j + g_j \delta S_{jj+1} + \sqrt{2\kappa_j} \delta a_j^{\text{in}}, \\ \frac{d}{dt} \delta S_{11} &= \gamma_1 \delta S_{22} + g_1 (\langle S_{21} \rangle \delta a_1 + \langle a_1 \rangle \delta S_{21} + \text{H.c.}) \\ &+ \sqrt{\gamma_1/N} (S_{21} B_1^{\text{in}} + B_1^{\text{in}\dagger} S_{12}), \end{aligned}$$

$$\begin{aligned} \frac{d}{dt} \delta S_{33} &= -\gamma_2 \delta S_{33} - g_2 (\langle S_{32} \rangle \delta a_2 + \langle a_2 \rangle \delta S_{32} + \text{H.c.}) \\ &- \sqrt{\gamma_2/N} (S_{32} B_2^{\text{in}} + B_2^{\text{in}\dagger} S_{23}), \end{aligned} \quad (24)$$

$$\begin{aligned} \frac{d}{dt} \delta S_{12} &= -\frac{\gamma_1}{2}(1+i\Delta_{21})\delta S_{12} + g_1 \langle a_1 \rangle (\delta S_{22} - \delta S_{11}) \\ &+ g_1 (\langle S_{22} \rangle - \langle S_{11} \rangle) \delta a_1 + g_2 \langle a_2^\dagger \rangle \delta S_{13} \\ &+ g_2 \langle S_{13} \rangle \delta a_2^\dagger + \sqrt{\gamma_1/N} (S_{22} - S_{11}) B_1^{\text{in}} \\ &+ \sqrt{\gamma_2/N} B_2^{\text{in}\dagger} S_{13}, \end{aligned}$$

$$\begin{aligned} \frac{d}{dt} \delta S_{23} &= -\frac{1}{2}(\gamma_1+\gamma_2)(1+i\Delta_{32})\delta S_{23} - g_1 \langle a_1^\dagger \rangle \delta S_{13} \\ &- g_1 \langle S_{13} \rangle \delta a_1^\dagger + g_2 \langle a_2 \rangle (\delta S_{33} - \delta S_{22}) \\ &+ g_2 (\langle S_{33} \rangle - \langle S_{22} \rangle) \delta a_2 - \sqrt{\gamma_1/N} B_1^{\text{in}\dagger} S_{13} \\ &+ \sqrt{\gamma_2/N} (S_{33} - S_{22}) B_2^{\text{in}}, \end{aligned}$$

$$\begin{aligned} \frac{d}{dt} \delta S_{13} &= -\frac{\gamma_2}{2}(1+i\Delta_{31})\delta S_{13} + g_1 \langle a_1 \rangle \delta S_{23} \\ &+ g_1 \langle S_{23} \rangle \delta a_1 - g_2 \langle a_2 \rangle \delta S_{12} - g_2 \langle S_{12} \rangle \delta a_2 \\ &+ \sqrt{\gamma_1/N} S_{23} B_1^{\text{in}} - \sqrt{\gamma_2/N} S_{12} B_2^{\text{in}}, \end{aligned}$$

and

$$\delta S_{11} + \delta S_{22} + \delta S_{33} = 0. \quad (25)$$

Note that the atomic operators themselves occur in the noise terms. This is of relevance when we calculate the noise-correlation matrix using the operator multiplication rules.

Using the following method due to Gheri [17], we are now able to calculate all the fields and atoms correlations. A similar method in the frequency domain is presented in Ref. [18]. We can write the whole linearized system [(24)

ing of the difference of the two output fields, and compare the results with the results obtained in a previous publication [14] using effective two-level atoms. For this effective two-level model, the one-photon detunings were assumed to be very large. Here we shall find out how large Δ_{21} has to be for the effective two-level model to be valid.

The squeezing spectrum for the quadrature component

$$X(\alpha, t) = \delta a^{\text{out}}(t) e^{-i\alpha} + \delta a^{\text{out}\dagger}(t) e^{i\alpha} \quad (34)$$

is defined for $t \rightarrow \infty$ by

$$V(\alpha, \omega) = \int_{-\infty}^{\infty} e^{-i\omega\tau} \langle X(\alpha, t + \tau) X(\alpha, t) \rangle d\tau. \quad (35)$$

From now on, in order to simplify the notation, we shall omit the δ in front of the operators. And since we are interested in the stationary regime, the time t is irrelevant and will be omitted.

The expanded expression for the squeezing spectrum is the following:

$$\begin{pmatrix} \frac{1}{\sqrt{N}} \left[\left[\frac{\kappa_1}{\kappa_1 + \kappa_2} \right]^{1/2} e^{-i\theta_1^{\text{out}}} a_1 + \left[\frac{\kappa_2}{\kappa_1 + \kappa_2} \right]^{1/2} e^{-i\theta_2^{\text{out}}} a_2 \right] \\ \frac{1}{\sqrt{N}} \left[\left[\frac{\kappa_1}{\kappa_1 + \kappa_2} \right]^{1/2} e^{i\theta_1^{\text{out}}} a_1^\dagger + \left[\frac{\kappa_2}{\kappa_1 + \kappa_2} \right]^{1/2} e^{i\theta_2^{\text{out}}} a_2^\dagger \right] \\ \frac{1}{\sqrt{N}} \left[\left[\frac{\kappa_1}{\kappa_1 + \kappa_2} \right]^{1/2} e^{-i\theta_1^{\text{out}}} a_1 - \left[\frac{\kappa_2}{\kappa_1 + \kappa_2} \right]^{1/2} e^{-i\theta_2^{\text{out}}} a_2^\dagger \right] \\ \frac{1}{\sqrt{N}} \left[\left[\frac{\kappa_1}{\kappa_1 + \kappa_2} \right]^{1/2} e^{i\theta_1^{\text{out}}} a_1^\dagger - \left[\frac{\kappa_2}{\kappa_1 + \kappa_2} \right]^{1/2} e^{i\theta_2^{\text{out}}} a_2^\dagger \right] \end{pmatrix} \quad (38)$$

and make the corresponding transformations on the \underline{A} matrix and the \underline{G} matrix. This new set of variables enables us now to compute the squeezing spectra using Eqs. (36) and (37) and the new \underline{C}_0 correlation matrix. The squeezing of the quadrature at angle α is given by

$$V(\alpha, \omega) = 1 + (\kappa_1 + \kappa_2) \left[(\underline{A} - i\omega \underline{I})^{-1} \underline{G} (\underline{A}^T + i\omega \underline{I})^{-1} + (\underline{A} + i\omega \underline{I})^{-1} \underline{G} (\underline{A}^T - i\omega \underline{I})^{-1} \right]_{i+1, i} - e^{2i\alpha} \{ 2 \underline{C}_0 \underline{A}^T [(\underline{A}^T)^2 + \omega^2 \underline{I}]^{-1} \}_{i+1, i+1} - e^{-2i\alpha} \{ (\underline{A}^2 + \omega^2 \underline{I})^{-1} 2 \underline{A} \underline{C}_0 \}_{i, i} \}, \quad (39)$$

where $i = 1$ for the sum, and $i = 3$ for the difference. \underline{I} is the identity matrix. The best squeezing spectrum is then expressed by

$$V_B(\omega) = 1 + (\kappa_1 + \kappa_2) \left[(\underline{A} - i\omega \underline{I})^{-1} \underline{G} (\underline{A}^T + i\omega \underline{I})^{-1} + (\underline{A} + i\omega \underline{I})^{-1} \underline{G} (\underline{A}^T - i\omega \underline{I})^{-1} \right]_{i+1, i} - 4 \{ \underline{C}_0 \underline{A}^T [(\underline{A}^T)^2 + \omega^2 \underline{I}]^{-1} \}_{i+1, i+1} \}. \quad (40)$$

IV. RESULTS

We first consider the parameters corresponding to the practical case of a sodium atom to find out whether the effective two-level atom discussed in a previous publication [14] is still valid. We have plotted in Fig. 2 the best difference squeezing spectrum obtained with the effective two-level model and the spectrum given by the present analysis with the two one-photon atom-cavity couplings g_1 and g_2 of equal magnitude giving the same two-photon coupling $g = g_1 g_2 / \Delta_{21}$. This is the situation corresponding to the levels $3s_{1/2} - 3p_{3/2} - 3d_{5/2}$ of the sodium atom

$$V(\alpha, \omega) = \int_{-\infty}^{\infty} e^{-i\omega\tau} \left[\langle a^{\text{out}\dagger}(\tau) a^{\text{out}} \rangle e^{2i\alpha} + \langle a^{\text{out}}(\tau) a^{\text{out}} \rangle e^{-2i\alpha} + \langle a^{\text{out}\dagger}(\tau) a^{\text{out}} \rangle + \langle a^{\text{out}}(\tau) a^{\text{out}\dagger} \rangle \right] d\tau. \quad (36)$$

We now have to relate these correlations involving the output field operators to the correlation matrix [Eq. (33)] for the internal-field operators. This can be done relatively easily using the input-output formalism [15]. For coherent inputs, we have (for $j = 1, 2$):

$$\langle a_j^{\text{out}\dagger}(\tau) a_j^{\text{out}} \rangle = 2\kappa_j \langle a_j^\dagger(\tau) a_j \rangle \quad (37)$$

and

$$\langle a_j^{\text{out}}(\tau) a_j^{\text{out}} \rangle = 2\kappa_j [\Theta(\tau) \langle a_j(\tau) a_j \rangle + \Theta(-\tau) \langle a_j a_j(\tau) \rangle].$$

Here we are interested in the best squeezing of the sum or the difference of the two output fields. It is therefore more convenient to define a new \mathbf{v} vector whose four first elements are

used in Grangier's QND experiment [12]. The third spectrum shows what happens when the one-photon coupling for the upper transition is weaker (which is the case in most situations), the two-photon coupling remaining the same by decreasing the one-photon detuning Δ_{21} . For all these three plots the total normalized phase shifts defined (for $j = 1, 2$) by

$$\Phi_j^{\text{tot}} = \Phi_j - \text{Im}[g_j S_{jj+1} / (\kappa_j \langle a_j \rangle)] \quad (41)$$

are taken equal to 0.6. It turns out that, for the configuration with identical one-photon atom-cavity cou-

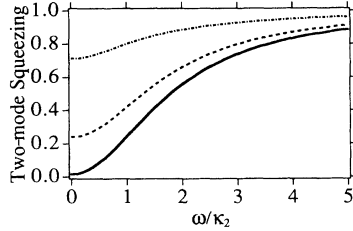


FIG. 2. Comparison of the best squeezing of the difference for the full three-level atom and for the effective two-level model. For all of these plots we have $\kappa_1 = \kappa_2 = 7 \times 10^6$ and $N = 5 \times 10^7$. The total normalized detunings Φ_{tot}^j (for $j=1,2$) are equal to 0.6. The solid line corresponds to the result given by the effective two-level model for a two-photon coupling of $g = 50$ with a two-photon detuning Δ_{31} of $100(\gamma_2/2)$ and equal intensities for both fields corresponding to $\langle a_1 \rangle = \langle a_2 \rangle = 337.4$. The dashed line is the spectrum given by the present full three-level analysis for parameters corresponding to the sodium atom used in the experiment of Grangier *et al.* [12]. We have $\gamma_1 = 6.13 \times 10^7$, $\gamma_2 = 5.03 \times 10^7$, $g_1 = g_2 = 10^6$, $\Delta_{31} = 100(\gamma_2/2)$, and $\Delta_{21} = -g_1 g_2 / g = -652.5(\gamma_2/2)$. The dash-dotted line is the spectrum for the same two-photon coupling in the more common case where the one-photon coupling for the upper transition is $\sqrt{10}$ times weaker ($g_2 = 10^6/\sqrt{10}$), the one-photon detuning $\Delta_{21} = -(652.5/\sqrt{10})(\gamma_2/2)$ also $\sqrt{10}$ times smaller and the relaxation rate 10 times smaller ($\gamma_2 = 5.03 \times 10^6$).

pling, the amount of squeezing is still acceptable (to 0.25 of the vacuum noise at zero frequency compared to almost perfect squeezing predicted by the effective two-level model), but when the coupling for the upper transition is weaker and Δ_{21} therefore smaller in order to compensate, the worsening of the squeezing is quite dramatic (to only 0.7 of the vacuum noise at zero frequency) and the effective two-level model is clearly no longer valid.

We then look at the behavior of the best squeezing at zero frequency in terms of the one-photon detuning Δ_{21} , the two-photon coupling g remaining constant. The one-photon atom-cavity couplings have therefore to be varied ($g_1 = g_2 = \sqrt{g|\Delta_{21}|}$) in order to compensate for the varia-

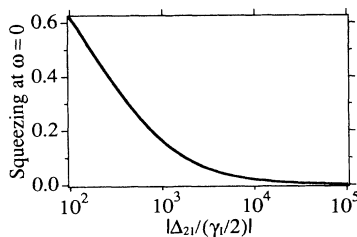


FIG. 3. Difference between the best squeezing value at zero frequency obtained with the three-level analysis and the one obtained with the effective two-level model for the same two-photon coupling ($g = 50$) and two-photon detuning $\Delta_{31} = 100(\gamma_2/2)$ in terms of the logarithm of the normalized one-photon detuning $|\Delta_{21}|/(\gamma_1/2)$. So $|\Delta_{21}|$ goes from $10^2(\gamma_1/2)$ to $10^5(\gamma_1/2)$. The parameters are $\kappa_1 = \kappa_2 = 7 \times 10^6$, $N = 5 \times 10^7$, $\gamma_1 = 6.13 \times 10^7$, $\gamma_2 = 5.03 \times 10^7$, and $\langle a_1 \rangle = \langle a_2 \rangle = 337.4$. In order to keep the two-photon coupling constant, we have $g_1 = g_2 = \sqrt{g|\Delta_{21}|}$.

tion of Δ_{21} . We have plotted in Fig. 3 the difference between the best squeezing at zero frequency of the two-mode difference obtained with the full three-level analysis and the value given by the effective two-level model. It can be seen that, for a two-photon detuning Δ_{31} of $100(\gamma_2/2)$, the effective two-level model is valid with an accuracy of a few percent only for a one-photon detuning Δ_{21} larger than $10^4(\gamma_1/2)$. These quite large detunings require one-photon atom-cavity couplings that are somewhat hard to achieve experimentally; typical one-photon detunings are in practice of the order of $10^3(\gamma_1/2)$, which still gives quite acceptable results.

V. QND MEASUREMENTS

We shall now evaluate the effectiveness of this system as a QND-measurement scheme using the criteria developed in Ref. [13]. The coefficients we want to calculate are all normalized correlations between two particular quadratures of the different input and output fields. In the general case, let us denote by $p(t)$ and $q(t)$ the two real quantities (i.e., Hermitian operators) we are interested in. We want to compute the following quantity:

$$C(\omega) = \frac{\left| \int_{-\infty}^{\infty} e^{-i\omega\tau} \langle p(\tau)q + qp(\tau) \rangle d\tau \right|^2}{\int_{-\infty}^{\infty} e^{-i\omega\tau_p} \langle p(\tau_p)p \rangle d\tau_p \int_{-\infty}^{\infty} e^{-i\omega\tau_q} \langle q(\tau_q)q \rangle d\tau_q} \quad (42)$$

The three coefficients defined further on are of this type. But in order to simplify the notation, we just write them

$$C = \frac{|\langle pq \rangle|^2}{\langle p^2 \rangle \langle q^2 \rangle} \quad (43)$$

The first coefficient tells us how accurately we can determine the signal input by measuring the probe output. This is quantified by the correlation coefficient C_1 defined by

$$C_1 = \frac{|\langle X^{\text{in}} Y^{\text{out}} \rangle|^2}{\langle X^{\text{in}2} \rangle \langle Y^{\text{out}2} \rangle}, \quad (44)$$

where X^{in} is the noise part ($\langle X^{\text{in}} \rangle = 0$) of the quadrature of the signal we want to measure, and Y^{out} the noise part of the quadrature of the probe we read. We have $0 \leq C_1 \leq 1$. For a perfect QND-measurement scheme $C_1 = 1$.

The second coefficient is a measure of how nondestructive the measurement scheme is. This is quantified by the correlation coefficient C_2 defined by

$$C_2 = \frac{|\langle X^{\text{in}} X^{\text{out}} \rangle|^2}{\langle X^{\text{in}2} \rangle \langle X^{\text{out}2} \rangle} \quad (45)$$

We have $0 \leq C_2 \leq 1$. If the measurement is perfectly nondestructive, $C_2 = 1$.

One requires a QND scheme to have better performance than the simple beam splitter [19]. The sum $C_1 + C_2$ gives a good indication of the ability of the scheme to perform QND measurements. We have

$C_1 + C_2 = 1$ for the simple beam splitter and $C_1 + C_2 = 2$ for a perfect QND-measurement scheme. So quantum effects are to be found within this interval.

The third coefficient tells us how good the scheme is as a state-preparation device. A good indicator for this is the variance in the signal output, given a measured value for the probe field. We first define the correlation coefficient C_3 by

$$C_3 = \frac{|\langle X^{\text{out}} Y^{\text{out}} \rangle|^2}{\langle X^{\text{out}^2} \rangle \langle Y^{\text{out}^2} \rangle}. \quad (46)$$

The conditional variance of the signal output, given a measured value of the probe field, is (for a linearized system):

$$V_C(X^{\text{out}}|Y^{\text{out}}) = \langle X^{\text{out}^2} \rangle (1 - C_3). \quad (47)$$

For a perfect state-preparation device $V_C(X^{\text{out}}|Y^{\text{out}}) = 0$, whereas for the beam splitter $V_C(X^{\text{out}}|Y^{\text{out}}) = 1$.

In order to get C_1 and C_2 , we need to work out correlations between the input and output operators. The boundary condition [Eq. (18)] enables us to do that the same way as we previously did in Eq. (50). We only consider the case where the input beams are in a coherent state.

The correlations we need for C_1 when field 1 is the signal and field 2 is the probe are

$$\begin{aligned} \langle a_2^{\text{out}}(\tau) a_1^{\text{in}} \rangle &= 0, \\ \langle a_2^{\text{out}\dagger}(\tau) a_1^{\text{in}\dagger} \rangle &= -2\sqrt{\kappa_1 \kappa_2} \Theta(\tau) \langle [a_2^\dagger(\tau), a_1^\dagger] \rangle, \\ \langle a_2^{\text{out}\dagger}(\tau) a_1^{\text{in}} \rangle &= 0, \\ \langle a_2^{\text{out}}(\tau) a_1^{\text{in}\dagger} \rangle &= -2\sqrt{\kappa_1 \kappa_2} \Theta(\tau) \langle [a_2(\tau), a_1^\dagger] \rangle. \end{aligned} \quad (48)$$

The correlations we need for C_2 are (for $j = 1, 2$)

$$\begin{aligned} \langle a_j^{\text{out}}(\tau) a_j^{\text{in}} \rangle &= 0, \\ \langle a_j^{\text{out}\dagger}(\tau) a_j^{\text{in}\dagger} \rangle &= -2\kappa_j \Theta(\tau) \langle [a_j^\dagger(\tau), a_j^\dagger] \rangle, \\ \langle a_j^{\text{out}\dagger}(\tau) a_j^{\text{in}} \rangle &= 0, \\ \langle a_j^{\text{out}}(\tau) a_j^{\text{in}\dagger} \rangle &= \delta(\tau) - 2\kappa_j \Theta(\tau) \langle [a_j(\tau), a_j^\dagger] \rangle. \end{aligned} \quad (49)$$

And for C_3 we need (for $j = 1, 2$)

$$\begin{aligned} \langle a_1^{\text{out}}(\tau) a_2^{\text{out}} \rangle &= 2\sqrt{\kappa_1 \kappa_2} [\Theta(\tau) \langle a_1(\tau) a_2 \rangle \\ &\quad + \Theta(-\tau) \langle a_2 a_1(\tau) \rangle], \\ \langle a_1^{\text{out}\dagger}(\tau) a_2^{\text{out}} \rangle &= 2\sqrt{\kappa_1 \kappa_2} \langle a_1^\dagger(\tau) a_2 \rangle, \\ \langle a_1^{\text{out}}(\tau) a_2^{\text{out}\dagger} \rangle &= 2\sqrt{\kappa_1 \kappa_2} \langle a_2^\dagger a_1(\tau) \rangle, \\ \langle a_1^{\text{out}\dagger}(\tau) a_2^{\text{out}\dagger} \rangle &= 2\sqrt{\kappa_1 \kappa_2} [\Theta(\tau) \langle a_2^\dagger a_1^\dagger(\tau) \rangle \\ &\quad + \Theta(-\tau) \langle a_1^\dagger(\tau) a_2^\dagger \rangle]. \end{aligned} \quad (50)$$

These correlations will enable us to derive the correlation in the frequency domain using the correlation matrix \underline{C}_0 and Eq. (33) and compute the coefficient in which we are interested.

VI. RESULTS

We will present here results with parameters that are all accessible in the experiment of Grangier *et al.* [12]. In this experiment the signal is the amplitude of the input field corresponding to the lower transition, and the read out is done on the phase of the probe beam which corresponds to the upper transition (configuration 1). But we have also investigated an alternative configuration where the signal is the amplitude of the field corresponding to the upper transition, and the probe is the phase of the field corresponding to the lower transition (configuration 2).

Some ranges of parameters can be found where both configurations give quite good and similar results (Fig. 4). For these plots, the total phase shifts Φ_{tot}^j (for $j = 1, 2$) are taken equal to zero so that the lasers are on resonance with the nonlinear cavity. For the two graphs presented in Fig. 4, the one-photon detunings are about ten times as large as the two-photon detuning, the Rabi frequencies $\Omega_j^R = g_j \langle a_j \rangle / \gamma_j$ of both fields are equal, but the cavity decay rate corresponding to the lower transition is four times as large as the one corresponding to the upper transition. This asymmetry can be understood by the fact that the lower transition is noisier because almost all the population is in the lower level, leading to a relatively large one-photon absorption for the lower transition. And we do not want this noise to be stored in too narrow a cavity. The QND-measurement criterion $C_1 + C_2$ is in both cases above 1.8, which means that we have more than 80% quantum correlations. The conditional variance characterizing the state-preparation capabilities of

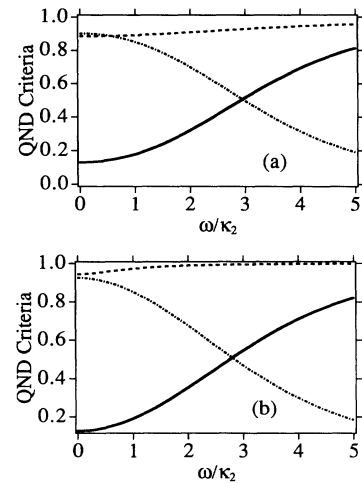


FIG. 4. QND criteria vs noise frequency when the total detunings Φ_{tot} are equal to zero. In (a) the signal is the lower transition while the probe is the upper one, while it is the other way around in (b). For both graphs the solid line is the conditional variance, the dash-dotted line is the measurement coefficient C_1 , and the dashed line is the signal-degradation coefficient C_2 . For both graphs the parameters are $N = 5 \times 10^7$, $\kappa_1 = 4\kappa_2 = 6.13 \times 10^7$, $\gamma_1 = 6.13 \times 10^7$, $\gamma_2 = 5.03 \times 10^7$, $g_1 = g_2 = 10^6$, $\langle a_1 \rangle = 1226$, $\langle a_2 \rangle = 1522$, $\Delta_{31} = -120(\gamma_2/2)$, and $\Delta_{21} = 1000(\gamma_1/2)$.

the system goes down to 0.12 in both cases, which is already a good result. However, it is possible to break the symmetry by taking parameters that will improve the performances of one configuration while the performances of the other one will be degraded. To achieve that for configuration 1, we take a strong signal with a Rabi frequency 20 times larger than for the probe. By doing that one can reach values of about 1.95 for $C_1 + C_2$ and a conditional variance of about 0.05, which is not far from the ideal QND situation.

From an experimental point of view, it may be more convenient to operate the probe at a nonzero frequency in order to get away from the experimental noise around zero frequency, and also to use the probe cavity as an interferometer which will rotate the phase quadrature of the internal field that contains the information into the amplitude of the output field which does not require any homodyne detection. This point is analyzed in detail in Ref. [20]. The probe beam is detuned outside of the cavity bandwidth (three times the cavity bandwidth, for example) while the signal is maintained on resonance with its cavity which has a broad bandwidth (about four times as large as the probe cavity) in order to include the sideband that will be read by the probe. The sideband of the output-meter beam that resonates with the cavity will contain all the information whereas the other sideband will not get any information. Therefore, it does not matter any more whether we look at the amplitude $a(\omega) + a^\dagger(-\omega)$ or the phase $i[a(\omega) - a^\dagger(-\omega)]$, the same information is in both phase and amplitude. We have presented in Fig. 5 the results in configuration 1 for the two output quadratures with the same parameters as in Fig. 4. The maximum correlations occur now at $\omega/\kappa_2 = 3$ and even though they are not as good as in Fig. 4 at zero frequency, they are definitely better at the sideband-resonance frequency. At this frequency the correlations have the same magnitude for both quadratures. In Fig. 5(a) we are looking at the phase of the output of the probe, therefore nothing happens at zero frequency (where the output phase corresponds to internal amplitude). In Fig. 5(b) we are now looking at the amplitude of the output. The correlations are about the same at $\omega/\kappa_2 = 3$ but the probe still picks up a little bit of information at zero frequency where the output amplitude corresponds to the internal phase but is not resonant. If the probe cavity bandwidth is larger (and the signal cavity bandwidth is larger as well) the correlation tends to decrease at zero frequency because we are then further away from resonance.

VII. CONCLUSION

We have carried out in this paper a full analysis of the noise characteristics of a three-level atom in a ladder

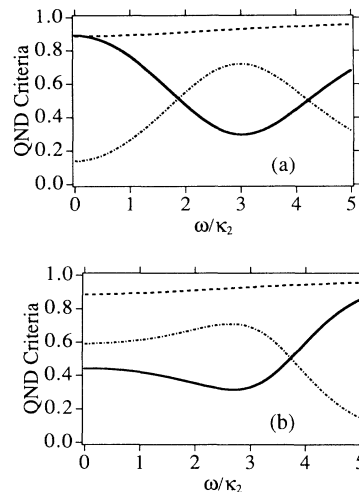


FIG. 5. QND criteria vs noise frequency in configuration 1 when the probe cavity is detuned from the probe by 3 cavity bandwidths ($\Phi_{\text{tot}}^2 = 3\kappa_2$). For both graphs, the solid line is the conditional variance, the dash-dotted line is the measurement coefficient C_1 , and the dashed line is the signal-degradation coefficient C_2 . In (a) we are looking at the probe phase output and in (b) at the probe amplitude output. All the parameters are the same as in Fig. 4.

configuration interacting with two cavity modes in the most general case (no assumption for the detunings and the field strength and no adiabatic elimination). We have used the input-output formalism of Gardiner and Collett [15] to get a set of quantum-stochastic differential equations that allowed us to compute the quantum correlations for this system. We have extended the results of a previous paper [14], on nondegenerate two-mode squeezing, analyzing the influence of a finite detuning with the intermediate level. We have then investigated the QND capability of this scheme already used experimentally by Grangier *et al.* [12] and we have shown that it can produce very good QND performances.

ACKNOWLEDGMENTS

We wish to thank K. M. Gheri, S. M. Tan, and P. Grangier for fruitful discussions. One of us (J.P.P.) was supported by the French Ministry of Foreign Affairs. This research was supported by the Auckland University Research Committee and the New Zealand Vice Chancellors Committee.

*Permanent address: Institut d'Optique, Boîte Postale 147, 91403 Orsay, France.

[1] C. M. Caves, K. S. Thorne, R. W. P. Drever, V. D. Sandberg, and M. Zimmermann, *Rev. Mod. Phys.* **52**, 341 (1980).

[2] G. J. Milburn and D. F. Walls, *Phys. Rev. A* **28**, 2065 (1983).

[3] N. Imoto, H. A. Haus, and Y. Yamamoto, *Phys. Rev. A* **32**, 2287 (1985).

[4] B. Yurke, *J. Opt. Soc. Am. B* **2**, 732 (1986).

- [5] R. M. Shelby and M. D. Levenson, *Opt. Commun.* **64**, 553 (1987).
- [6] P. Alsing, G. J. Milburn, and D. F. Walls, *Phys. Rev. A* **37**, 2970 (1988).
- [7] H. A. Bachor, M. D. Levenson, D. F. Walls, S. H. Perlmuter, and R. M. Shelby, *Phys. Rev. A* **38**, 180 (1988).
- [8] P. Grangier, J. F. Roch, and S. Reynaud, *Opt. Commun.* **72**, 387 (1989).
- [9] C. A. Blockley and D. F. Walls, *Opt. Commun.* **79**, 241 (1990).
- [10] M. D. Levenson, R. M. Shelby, M. D. Reid, and D. F. Walls, *Phys. Rev. Lett.* **57**, 2473 (1986).
- [11] A. La Porta, R. E. Slusher, and B. Yurke, *Phys. Rev. Lett.* **62**, 28 (1989).
- [12] P. Grangier, J. F. Roch, and G. Roger, *Phys. Rev. Lett.* **66**, 1418 (1991).
- [13] M. J. Holland, M. J. Collett, D. F. Walls, and M. D. Levenson, *Phys. Rev. A* **42**, 2995 (1990).
- [14] J. P. Poizat, M. J. Collett, and D. F. Walls, *Opt. Commun.* **84**, 409 (1991).
- [15] C. W. Gardiner and M. J. Collett, *Phys. Rev. A* **31**, 3761 (1985).
- [16] A. W. Boone and S. Swain, *Quantum. Opt.* **1**, 27 (1989).
- [17] K. M. Gheri (private communication).
- [18] J. M. Courty, P. Grangier, L. Hilico, and S. Reynaud, *Opt. Commun.* **83**, 251 (1991).
- [19] The correlation coefficients for a simple beam splitter (no squeezed vacuum) with a amplitude reflection coefficient of ν are $C_1 = \nu^2$, $C_2 = 1 - \nu^2$, $VC = 1$.
- [20] P. Grangier and J. F. Roch, *Opt. Commun.* **83**, 269 (1991).